NJC

Accepted Manuscript

This is an *Accepted Manuscript*, which has been through the Royal Society of Chemistry peer review process and has been accepted for publication.

Accepted Manuscripts are published online shortly after acceptance, before technical editing, formatting and proof reading. Using this free service, authors can make their results available to the community, in citable form, before we publish the edited article. We will replace this *Accepted Manuscript* with the edited and formatted *Advance Article* as soon as it is available.

You can find more information about *Accepted Manuscripts* in the Information for Authors.

Please note that technical editing may introduce minor changes to the text and/or graphics, which may alter content. The journal's standard Terms & Conditions and the Ethical guidelines still apply. In no event shall the Royal Society of Chemistry be held responsible for any errors or omissions in this *Accepted Manuscript* or any consequences arising from the use of any information it contains.

ROYAL SOCIETY OF CHEMISTRY

www.rsc.org/njc

Cite this: DOI: 10.1039/c0xx00000x

www.rsc.org/xxxxxx

ARTICLE TYPE

V_2O_5/SBA-15 nanocatalysts for the selective synthesis of 2,3,5-trimethyl-1,4-benzoquinone at room temperature

Chinna Krishna Prasad Neeli, Venkata Siva Prasad Ganjala, Venkateswarlu Vakati, Kamaraju Seetha Rama Rao and David Raju Burri*

Received (in XXX, XXX) Xth XXXXXXXXX 20XX, Accepted Xth XXXXXXXXX 20XX
DOI: 10.1039/b000000x

A series of four V_2O_5/SBA-15 catalysts with the loadings of 5, 7.5, 10 and 12.5% (by weight) V_2O_5 have been prepared by molecular designed dispersion (MDD) method and are characterized by N_2-physisorption, low-angle and wide-angle XRD, transmission electron microscope (TEM), Fourier Transform-Raman spectroscopy (FT-Raman), Ultraviolet -Visible diffuse reflectance spectroscope (UV-Vis, DRS), temperature programmed reduction (TPR) and inductively coupled plasma - optical emission spectrometer (ICP-OES) techniques. Among V_2O_5/SBA-15 catalysts, 10%V_2O_5/SBA-15 catalyst exhibited 99% 2,3,5-trimethylphenol (TMP) conversion with 95% 2,3,5-trimethyl-1,4-benzoquinone (TMBQ) yield when H_2O_2 (30% aqueous solution) and ethanol were used as green oxidant and green solvent respectively at room temperature. The remarkable activity of 10%V_2O_5/SBA-15 catalyst is due to isolated distribution of uniformly sized nanovanadium species on the pore surfaces of hexagonally ordered mesoporous SBA-15 silica support.

Introduction

Vitamins are essential food components which are either not synthesized in the human or animal organism or not formed in sufficient amounts. Selective oxidation of phenols to quinones constitutes an essential biological process [1] and is of significant interest to the chemical industry.[2] Quinones serve as electron acceptors in electron transport chains in photosynthesis and aerobic respiration.[3] Among the industrially relevant quinones, TMBQ represents a crucial intermediate for the industrial synthesis of α-tocopherol that is the most active component of vitamin E,[4] which is of particular economical relevance and industrial interest, extensively used as antioxidant in food, medical treatments and cosmetics.[5]

Notably, TMBQ provides the anti-aging properties, functions as anti-free radical thus acting to prevent apoplexy, heart disease, cardiovascular vessel disease and cancer.[6] Adequately, it shows biological properties such as antigerminative, antibacterial, antitumor, and antiprotozoan activities. In general, the main route for TMBQ production is *p*-sulphonation of TMP followed by stoichiometric oxidation with MnO_2.[7] Industrially, for the production of TMBQ copper halides and other copper salts/O_2 systems have been employed.[8] Catalytic systems such as cobalt (II) salen complexes, ruthenium salts and heteropolyacid systems using O_2 or H_2O_2 are reported.[9-11] However, the main drawback of the above mentioned systems is the use of homogeneous catalysts which leads to the problem of catalyst separation, recycling and product purification.

Evidently, there has been a rising demand for economic and environmentally friendly processes, requires the development of clean oxidation methods. Nowadays, green chemistry has become the central issue in both academia and industry as a sustainable approach for fine chemical synthesis. [12] Aqueous H_2O_2 is an ideal, inexpensive, very attractive, and waste-avoiding oxidant for liquid phase reactions [13] which gained particular interest from the point of "green" chemistry, with generation of H_2O as the only co-product.

To date, titanium silicates TS-1 and TS-2 are effective catalysts for H_2O_2 based heterogeneous oxidation [14] and have undergone continuous development. However, the use of these catalysts is limited to compounds with a kinetic diameter less than 6 Å and inefficient for the selective oxidation of bulky reactants due to slow diffusion of reactants and/or products and deactivation caused by substance blockage in micropores. It is therefore reasonable to research the elaboration of new environmental friendly catalysts with greater porosity and host the larger molecules.

Oxovanadium species have been found to have particular catalytic activity especially in oxidation reactions.[15] The presence of V^{+5} dimers or small oligomers with adjacent V atoms is required to ensure fast oxidation. Synthesis of supported and unsupported nanovanadium catalysts have been synthesized and discussed the structural features.[16-22] Herein, V_2O_5/SBA-15 nanovanadium catalysts have been prepared by MDD method and the superior performance of these nanocatalysts in the oxidation

of 2,3,5-trimethylphenol to 2,3,5-trimethyl-1,4-benzoquinone has been described.

Experimental

Catalyst preparation

The siliceous SBA-15 was synthesized in accordance with the literature procedures.[23, 24] A solution of $EO_{20}PO_{70}EO_{20}$:2 M HCl: TEOS: H_2O = 2:60:4.25:15 (mass ratio) was prepared, stirred for 12 h at 40 °C and then hydrothermally treated at 100 °C under static condition for 12 h, subsequently filtered, dried at 100 °C and calcined at 550 °C for 8 h, the yielded white powder is mesoporous silica SBA-15, which is used as a support, it is also known as a parent SBA-15. To prepare mesoporous SBA-15 supported nanovanadium catalysts (V_2O_5/SBA-15), deposition of $VO(acac)_2$ metal complexes onto the SBA-15 surface was performed by the liquid phase MDD method.[22] With slight modification of MDD method, the V_2O_5/SBA-15 catalysts were prepared wherein, requisite amounts of $VO(acac)_2$ was dissolved in 100 ml of dry dichloromethane solution with simultaneous addition of vaccum dried SBA-15 support (120 °C for 6 h) followed by stirring for 1 h at room temperature. The resultant slurry was filtered off, washed thoroughly with toluene and dried at 100 °C for 12 h. The acac ligands were removed by calcination, which was performed in a programmable oven at 450 °C for 5 h in air and represented as xV_2O_5/SBA-15 catalysts where prefixed x indicates the loading of V_2O_5 (by weight %).

Catalyst characterization

The X-ray diffraction (XRD) patterns were recorded at room temperature using an X-ray diffractometer (Multiflex, M/s. Rigaku, Japan) with a nickel filtered CuKα radiation. N_2 adsorption–desorption isotherms were recorded on a N_2 adsorption unit at -196 °C (Quadrasorb-SI V 5.06, M/s. Quantachrome Instruments Corporation, USA). The samples were out-gassed at 200 °C for 4 h prior the measurement. FT-Raman spectra were recorded on a Nicolet Nexus FT-Raman spectrometer with a Ge detector. All samples were measured at room temperature in 180° reflective sampling configuration, with 1064 nm Nd:YAG excitation laser. For each spectrum, 2.0 scans were averaged and the laser power was set between 1 and 2 W. TEM images were taken on a Philips Technai G2 FEI F12 instrument at an accelerating voltage of 80-100 kV. The samples were crushed in A.R. grade ethanol and the resulting suspension was allowed to dry on carbon film supported on copper grids. UV–Vis DRS were recorded at room temperature using a UV-2000 spectrophotometer (M/s Shimadzu, Japan) equipped with a diffuse reflectance attachment with an integrating sphere containing $BaSO_4$ as a reference. The spectra were recorded in the range 200-800 nm with sampling interval of 0.5 nm and slit width of 2 nm. The TPR profiles of the catalysts were obtained from a homemade apparatus consisting of TCD equipped GC and a quartz microreactor. In a typical TPR experiment, the fixed bed quartz microreactor was loaded with 50 mg of catalyst and raised the temperature in the flow of 5% H_2 in Argon (v/v) with a heating rate of 10 ºC/min from room temperature to 800 °C and hold at this temperature for 30 min to ensure the complete reduction. The elemental composition was carried over ICP-OES analysis (iCAP6500 series, M/s. Thermo Scientific, Germany).

Liquid phase oxidation of 2,3,5-trimethylphenol

In a typical experiment, 50 mg of V_2O_5/SBA-15 nanocatalyst was dispersed in 2 ml of ethanol (EtOH) in 10 ml capacity round bottomed flask, which was open to air. Subsequently, 1 mmol of 2,3,5-trimethylphenol and 3 mmol of H_2O_2 (30% aqueous solution) were added and reaction was conducted at room temperature under constant stirring for 1h. After completion of the reaction, the catalyst was separated from the product mixture by simple filtration, dried over anhydrous $MgSO_4$ to remove water and analyzed by a gas chromatograph (GC-17A, M/s. Shimadzu Instruments, Japan) using an Equity-5 capillary column (0.53 mm x 30 m). The products were confirmed by GC-MS (QP-5050 model, M/s. Shimadzu Instruments, Japan) equipped with DB-5 capillary column (0.32 mm dia. and 25 m long, M/s. J & W Scientific, USA).

Results and Discussion

ICP-OES

To confirm the loading of vanadium, all the four V_2O_5/SBA-15 catalysts were analyzed by ICP-OES and displayed the data in the parenthesis against each catalyst Viz., $5V_2O_5$/SBA-15(4.9wt%), $7.5V_2O_5$/SBA-15(8.5wt%), $10V_2O_5$/SBA-15(10.7wt%) and $12.5V_2O_5$/SBA-15(12.8wt%).

X-Ray Diffraction

To assess the mesoporous nature of V_2O_5/SBA-15 catalysts including SBA-15, low angle XRD analysis was made and the obtained patterns were shown in Fig. 1. The parent SBA-15 exhibited three well-resolved peaks at 2θ = 0.96, 1.65 and 1.90°

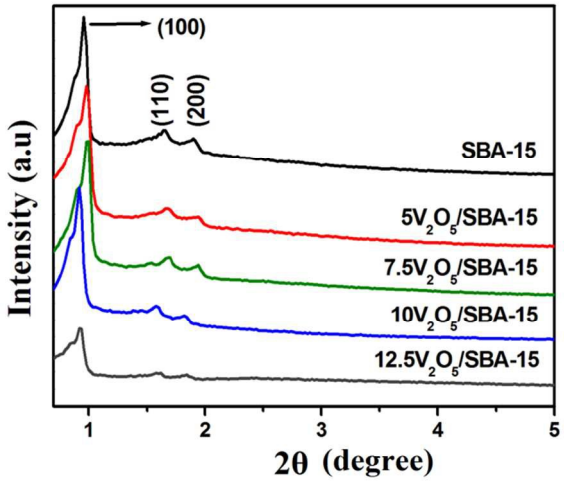

Fig. 1 Low-angle XRD patterns of SBA-15 and V_2O_5/SBA-15 catalysts.

indexed as (100), (110) and (200) reflections, characteristic of two-dimensional (2D) hexagonal mesostructure with *p6mm* space group. Similar to SBA-15, V_2O_5/SBA-15 catalysts also exhibited three diffraction peaks positioned at 0.91–0.96°, 1.57–1.69°, and 1.81–1.95°, revealing the retention of well ordered mesoporous nature of SBA-15 in all the prepared V_2O_5/SBA-15 catalysts.

To evaluate the crystalline behaviour of vanadium oxide species that dispersed on the surface of SBA-15 support, the V_2O_5/SBA-15 catalysts were characterized by wide-angle XRD

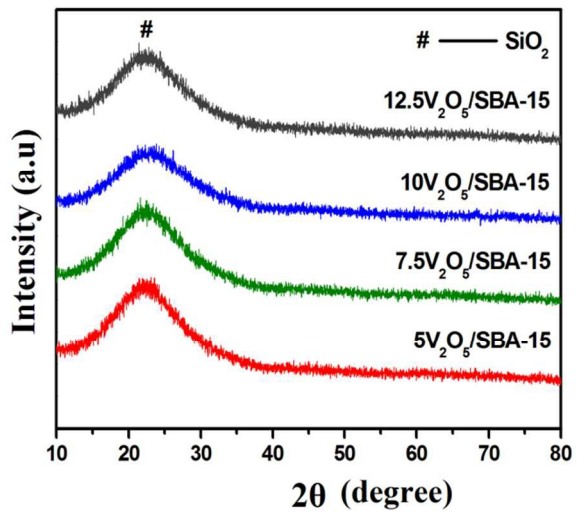

Fig. 2 Wide-angle XRD patterns of various V_2O_5/SBA-15 catalysts.

in the 2θ range of 10-80° (Fig. 2). A broad peak that appears in all the patterns at 2θ ≈ 22° is responsible for the SiO_2 phase of SBA-15. The absence of characteristic V_2O_5 XRD peaks at all the loadings of V_2O_5/SBA-15 catalysts may be due to higher dispersion of nanovanadium oxide with crystallite size less than 5 nm (XRD detection limit) or its presence on SBA-15 as amorphous phase.

N_2-Physisorption studies

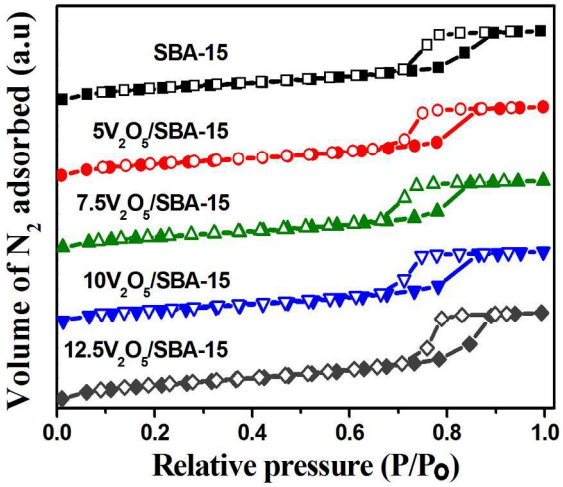

Fig. 3 N_2 adsorption-desorption isotherms of SBA-15 and various V_2O_5/SBA-15 catalysts.

Figure 3 shows the V_2O_5/SBA-15 catalysts, together with the parent SBA-15 are characterized by N_2 adsorption-desorption measurements. The isotherms obtained for parent SBA-15 and V_2O_5/SBA-15 catalysts are of type IV in nature with H1 hysteresis loop and well defined step due to capillary condensation in the range 0.6–0.8 p/p_0 in accordance with the IUPAC classification is typical nature of ordered mesoporous materials with cylindrical pores in a narrow pore size distribution. All V_2O_5/SBA-15 catalysts show hysteresis loops similar to that of parent SBA-15, implying the retention of mesophase structure.

Table 1. Textural and structural parameters of V_2O_5/SBA-15 catalysts from N_2 sorption data and low angle XRD analysis.

Catalyst	S_{BET}[a] ($m^2 g^{-1}$)	V_t[b] ($cm^3 g^{-1}$)	D[c] (nm)	d_{100}[d] (nm)	a_o[e] (nm)	t[f] (nm)
SBA-15	762	1.19	8.14	9.18	10.6	2.4
$5V_2O_5$/SBA-15	538	0.84	7.95	9.01	10.4	2.4
$7.5V_2O_5$/SBA-15	511	0.80	7.10	8.95	10.3	3.2
$10V_2O_5$/SBA-15	546	0.85	7.91	9.65	11.1	3.2
$12.5V_2O_5$/SBA-15	625	1.04	7.99	9.46	10.9	2.9

[a] BET surface area. [b] Total pore volume. [c] BJH average pore diameter. [d] Periodicity of (100) plane. [e] Unit cell length (a_0=2 $d_{(100)}/\sqrt{3}$). [f] Pore wall thickness ($t=a_0- D_{BJH}$).

The structural and textural parameters are summarized in Table 1. The specific surface area and total pore volume of parent SBA-15 decreased as the loading of active V_2O_5 component increased, which is ascertained from the partial blockage of pore mouths. The marginal increment in the surface area in the case of higher loading catalysts such as $10V_2O_5$ and $12.5V_2O_5$ catalysts may be due to segregation of certain particulates of V_2O_5 phase.[25] Fig. 4 shows the pore size distribution curves of V_2O_5/SBA-15 catalysts, which reveals that most of the pores are distributed in the range of 6-10 nm.

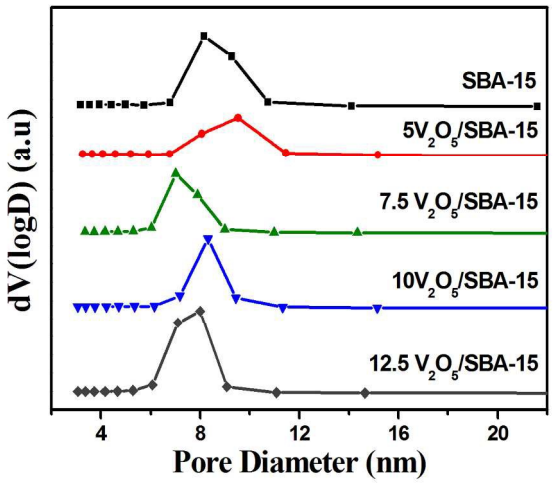

Fig. 4 Pore size distribution curves of various V_2O_5/SBA-15 catalysts.

FT-Raman spectroscopy

Raman spectroscopy is a very interesting characterization tool as it is very sensitive to the presence of crystals, even if in XRD, V_2O_5 crystallites are not seen, FT-Raman would give typical bands of these crystals. Fig. 5 shows the laser Raman spectra ranging from 1200 cm^{-1} to 200 cm^{-1} of all the samples. A clear band at 1036 cm^{-1} attributed to symmetric V=O stretching vibrations of isolated distorted vanadium tetrahedron (VO_4) species [26] in a well dispersed way. The absence of a typical band at 995 cm^{-1} in spectra a–c implies that no crystalline V_2O_5 was observed in all the samples which indicate V_2O_5 is highly dispersed in the mesoporous silica-based SBA-15 catalyst and

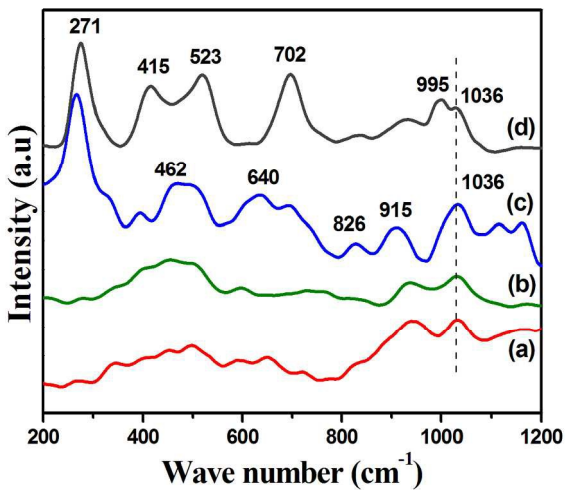

Fig. 5 Raman spectra of (a) $5V_2O_5$/SBA-15 (b) $7.5V_2O_5$/SBA-15 (c) $10V_2O_5$/SBA-15 and (d) $12.5V_2O_5$/SBA-15 catalysts.

well supported by wide-angle XRD results. Whereas, a shoulder peak at 995 cm^{-1} in spectra of sample d indicates the formation of crystalline and/or microcrystalline nature of V_2O_5 species that may results the decrease in catalytic activity. The increase in the intensity of weak band at 915 cm^{-1} with increase in vanadium loading is characteristic of $Si(-O^-)_2$ functionalities corresponding to perturbation in silica vibrations indicating the formation of V-O-Si bands. The bands at 702, 523 and 271 cm^{-1} are assigned to VOx clusters.[26d] The bands at 462 cm^{-1} can be assigned to cyclic tetrasiloxane rings of the silica support, weaker bands appear at 640 and 826 cm^{-1} are attributed to cyclic trisiloxane rings and the symmetrical Si-O-Si stretching mode, respectively.[27]

TEM analysis

The TEM image (Fig. 6) of $10V_2O_5$/SBA-15 catalyst gives direct observation about the structural investigations of V_2O_5 nanoparticles, which are high and uniformly dispersed inside the pore channels of SBA-15. The particle size distribution (PSD) bar graph as inset reveals that the V_2O_5 particles are around 5.5 nm size of peak maxima.

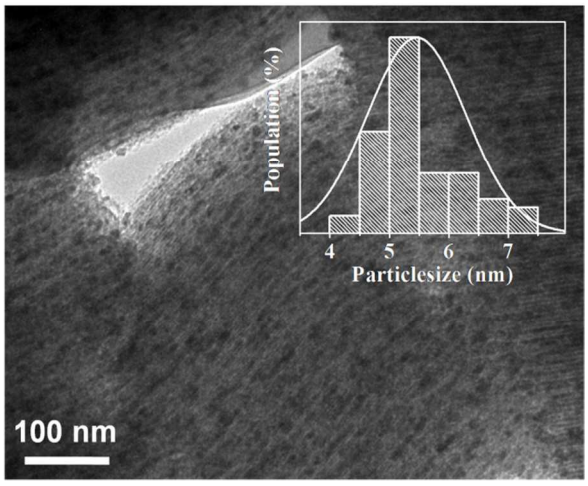

Fig. 6 TEM image of $10V_2O_5$/SBA-15 catalyst.

UV-Vis-DR spectra

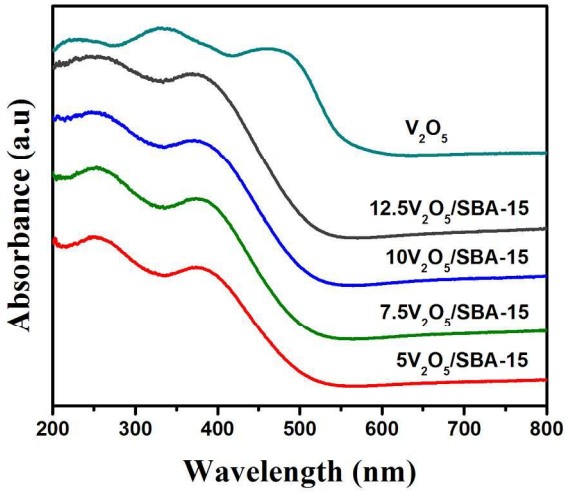

Fig. 7 UV-Vis-DR spectra of V_2O_5 and various V_2O_5/SBA-15 catalysts.

The room temperature UV-Vis-DR spectra of pure V_2O_5 and calcined V_2O_5/SBA-15 samples, additionally dried at 200 °C directly before the measurement, are presented in Fig. 7. The wide band between 240 and 300 nm observed for the $5V_2O_5$/SBA-15, $7.5V_2O_5$/SBA-15, $10V_2O_5$/SBA-15 and $12.5V_2O_5$/SBA-15 samples could be assigned to V^{5+} species in four fold coordination state of highly dispersed V_2O_5 species on the support surface, which were also detected by FT-Raman measurements. The additional peak in the range of 350-400 nm confirms the V^{5+} species in six fold coordination state and corresponds to low polymerized V chains or/and domains with V^{5+} species in square pyramidal configuration. The relative intensity of the band at 380 nm increased due to hydration of the V^{5+} species in tetrahedral coordination. However, even at the highest $12.5V_2O_5$/SBA-15 loading, absorption above 470 nm was not observed as in the case of pure V_2O_5 and therefore concluded the absence of microcrystalline V_2O_5 species in the studied catalysts.

Temperature Programmed Reduction

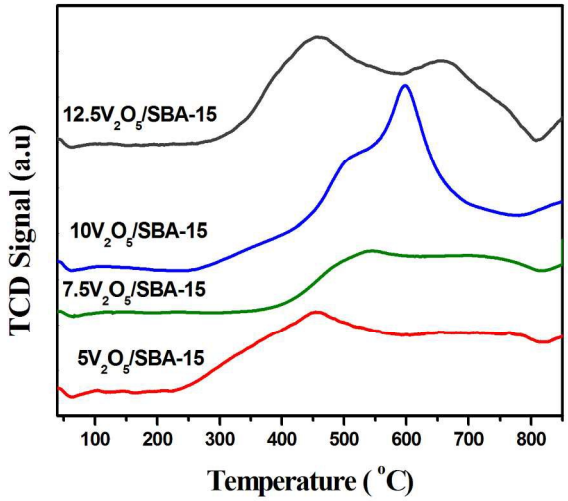

Fig. 8 H_2-TPR profiles of various V_2O_5/SBA-15 catalysts.

Temperature Programmed Reduction reveals the reducibility and stability of the metal/metal oxide supported catalysts and even surface distribution of different loadings of metal species. The TPR profiles of all the V_2O_5/SBA-15 samples between 100 and 800 °C with increasing vanadium loadings are comparatively shown in Fig. 8. For SBA-15 supported samples with V loadings from 5.0 to 10.0 wt%, the reduction temperature maximum in between 450-500 °C is attributed to the reduction of highly dispersed tetrahedral monomeric V_2O_5 species. An additional reduction temperature maximum in $10V_2O_5$/SBA-15 at 600 °C corresponds to the partially occluded tetrahedral V_2O_5 species by surface silica. In the case of $12.5V_2O_5$/SBA-15 with high V content, the main peak becomes broader shifted around 450 °C and the reduction temperature maximum shifted to higher temperature 658 °C, suggesting that polymeric vanadium species deposited on the high-surface area SBA-15 support that might be more difficult to reduce than isolated vanadium species under the TPR conditions. However, the smaller integral peak area of the $10V_2O_5$/SBA-15 than $12.5V_2O_5$/SBA-15 and the progressive shift of the maximum of the H_2 consumption peak to high temperature with the V loading suggests a progressive formation of less reducible high polymeric vanadium species which is also confirmed by a shoulder peak around 995 cm^{-1} in Raman spectra.

SEM-EDX Spectrum

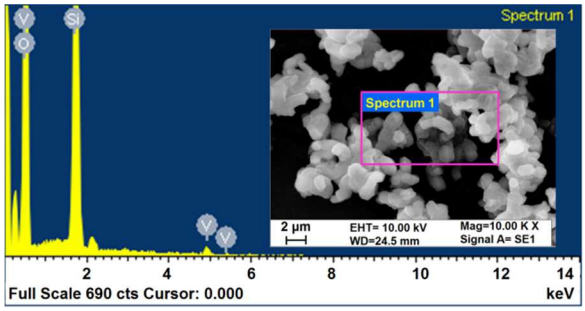

Fig. 9 SEM image of $10V_2O_5$/SBA-15 catalyst as inset in its EDX spectrum.

The morphology of the $10V_2O_5$/SBA-15 catalyst was confirmed by SEM analysis (Fig. 9 as inset) and EDX elemental mapping confirms the presence of nanovanadium species (Fig. 9).

Reaction scheme

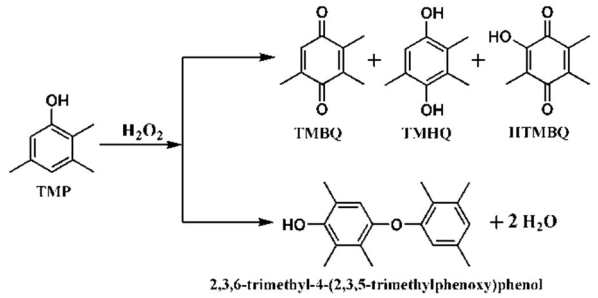

Scheme 1 Possibility of products in 2,3,5,-trimethylphenol Oxidation.

Despite the formation of several products such as 2,3,5-trimethylhydroquinone (TMHQ), 2-hydroxy-3,5,6-trimethyl-1,4-benzoquinone (HTMBQ) and 2,3,6-trimethyl-4-(2,3,5-trimethylphenoxy)phenol in the TMP oxidation (shown in scheme 1), selective formation of TMBQ is the present challenging task. To complete the task successfully, reaction parameters are systematically investigated.

Catalytic activity results

In our initial experiments, the influence of V_2O_5 loading on SBA-15 has been investigated using 50 mg of catalyst, 3 mmol of H_2O_2 (30% aqueous solution) and 1 mmol of TMP in EtOH (2 ml) at room temperature for 1 h. There observed a gradual increment in the conversion of TMP and selectivity of TMBQ with increase in V_2O_5 loading on SBA-15, which can be observed from Table 2. It seems that the formation of uniform sized particles of V_2O_5 and their isolated distribution on the high surface area SBA-15 are responsible for gradual increment in activity with increase V_2O_5 loading. Among different V_2O_5 loading catalysts, $10V_2O_5$/SBA-15 catalyst achieved good TMP conversion (63%) and TMBQ yield (49%), which seems to be the optimum loading catalyst. The catalytic activity of bulk V_2O_5 was evaluated (Table 2) and found to be inferior compared to present V_2O_5/SBA-15 nanocatalysts (Table 2).

Table 2. Effect of various wt% loadings of V_2O_5 over SBA-15 supported catalysts in the oxidation of TMP.

Loading (wt%)	TMP Conv. %	TMBQ Yield %	TMHQ Yield %
Bulk V_2O_5	15	11	04
$5V_2O_5$/SBA-15	22	15	07
$7.5V_2O_5$/SBA-15	50	34	16
$10V_2O_5$/SBA-15	63	49	14
$12.5V_2O_5$SBA-15	66	47	19

Other reaction parameters are optimized using $10V_2O_5$/SBA-15 catalyst. With increase in the 30% H_2O_2 to TMP molar ratio, from 2 to 3, the TMP conversion and TMBQ yield were increased from 54 to 63% and 41 to 49% that might be due to higher availability of oxidant molecules. A high TMP conversion 75% with TMBQ yield 64% was achieved at an oxidant to reactant mole ratio of 4. However, further increasing the amount of 30% H_2O_2, i.e., 4 to 5 mmol, no significant changes in the activity has been noticed. Hence, the optimum oxidant to substrate mole ratio is 4.

The influence of solvents was investigated, using different solvents and the results are shown in Table 3, which, reveals that the EtOH is the best solvent compared to others.

Table 3. Effect of solvents in the oxidation of TMP over $10V_2O_5$/SBA-15.

Solvent	TMP Conv. %	TMBQ Yield %	TMHQ Yield %
Toluene	05	03	02
Chloroform	10	07	03
Dichloromethane	13	05	08
Neat	19	11	08
Acetonitrile	62	48	14
Ethanol	75	64	11

The effect of amount of $10V_2O_5$/SBA-15 catalyst on the oxidation of TMP was studied using different amounts of catalyst viz., 25, 50, 75 and 100 mg. The increase in the amount of catalyst from 25 to 50 mg, augmentation in the TMP conversion from 68 to 75% and TMBQ yield 55 to 64% was observed. When 75 mg catalyst was used, the TMP conversion was raised to 87 % with TMBQ yield 78%. No significant changes either in the conversion or in the selectivity were observed beyond 75 mg of catalyst. Hence, the optimum amount of catalyst is 75 mg.

Table 4. Effect of time in the oxidation of TMP over $10V_2O_5$/SBA-15 catalyst.

Time (h)	TMP Conv. %	TMBQ Yield %	TMHQ Yield %
0.5	72	62	10
1.0	87	78	09
1.5	94	89	05
2.0	99	95	04

To understand the nature of $10V_2O_5$/SBA-15 towards the oxidation of TMP with reaction time, four different experiments were conducted and the results were displayed in Table 4. In the first half-an-hour experiment, the TMP conversion is 72% with the yield of TMBQ and TMHQ to 62 and 10%. In the 1 h experiment, the TMP conversion has been increased to 87% and TMBQ yield increased to 78%. Similar hike in activity has been observed in 1.5 h experiment, wherein the TMP conversion has been increased to 94% and TMBQ yield is to 89%. Notably, there was a decrease in the TMHQ yield from 09 to 05% with 1 to 1.5 h, which indicates the transformation of initially formed TMHQ to TMBQ product. Further in 2 h experiment, we achieved the maximum TMP conversion 99% and TMBQ yield 95%.

To test the heterogeneity of the catalyst, the TMP oxidation reaction was conducted using $10V_2O_5$/SBA-15 as a catalyst and 30% H_2O_2 as an oxidant at room temperature for 1 h and stopped the reaction and separated the catalyst from the reactant/product mixture and continued the reaction further 1, 2 and 3 h. No progress in the reaction after removing the catalyst was observed, revealing the absence of catalyst leaching and proving the reaction is in heterogeneous mode.

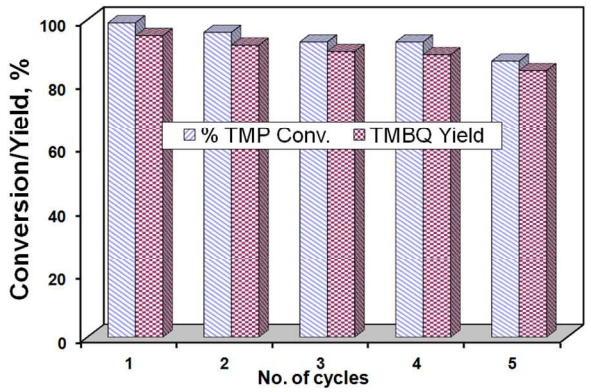

Fig. 10 Recyclability of $10V_2O_5$/SBA-15 catalyst.

To evaluate the reusability of the catalyst, a series of recycling experiments were conducted under optimised conditions and the results are depicted in Fig. 9, which reveals that there is no significant loss of catalytic activity on TMP oxidation up to 4 repeated cycles.

The present catalytic system, V_2O_5/SBA-15 prepared by MDD method is found to be a good catalyst for the oxidation of TMP to TMBQ at room temperature with 95% yield of TMBQ in the presence of green 30% H_2O_2 oxidant with eco-friendly ethanol solvent in 2 h. The similar high activity catalyst has also been reported, but at higher temperature. Kholdeeva and his co-workers contributed a lot for the oxidation of TMP to TMBQ over different catalysts such as mesostructured Ti-MMM[28] and TiO_2-SiO_2 aerogels.[29] The yield of TMBQ is 82% on both of these catalysts and observed hydrolytic instability of these catalysts. In the subsequent studies, the same group improved the thermal stability as well as catalytic activity up to 95% yield (at 80 ºC in acetonitrile solvent).[30-33] Very few reports are available on TMP oxidation at room temperature.[34] Unfortunately, the above systems involve the usage of environmentally undesirable solvent and operation at elevated temperatures which are the draw backs compared to present study. In the present research contribution, usage of hazardous chemical waste, stoichiometric amounts of oxidants and catalysts, harmful solvents, high temperatures operations linked to heating devices and electric power are avoided, which are the cutting-edge features of the present piece of work.

Conclusions

Molecular designed dispersion method yielded 4-7.5 nm sized V_2O_5/SBA-15 nanocatalysts, which are highly effective in the selective oxidation of trimethylphenol to trimethylbenzoquinone at room temperature and atmospheric pressure with green oxidant (30% H_2O_2) and eco-friendly ethanol solvent. The 10%V_2O_5/SBA-15 catalyst selectively oxidized trimethylphenol into trimethylbenzoquinone with 95% yield. The higher catalytic activities of V_2O_5/SBA-15 nanocatalysts are attributed to (i) uniformly sized V_2O_5 nanoparticles and (ii) their isolated distribution on the mesopore surfaces of hexagonally ordered porous catalysts, which are effective in providing intimate contact to the reactant molecules and diffusion-free environment to the products.

Acknowledgements

Chinna Krishna Prasad acknowledges the Council of Scientific and Industrial Research (CSIR-UGC) New Delhi, for awarding research fellowship. The authors thank Dr. R Nageswara Rao, Head Analytical Division, IICT, India, for their kind help with the ICP-OES analysis.

Notes and references

[a] *Catalysis Laboratory, Indian Institute of Chemical Technology, Hyderabad-500607. Fax: +91-40-27160921; Tel: +91-40-27191712; E-mail: david@iict.res.in*

1 (a) K. U. Baldenius, L. V. D. Bussche-Hnunefeld, E. Hilgemann, P. Hoppe and R. Sturmer, Ullmann's Encylopedia of Industrial Chemistry, VCH, Weinheim, 1996; (b) T. Dunlap, R. E. P.

Chandrasena, Z. Wang, V. Sinha, Z. Wang and G. R. J. Thatcher, *Chem. Res. Toxicol.*, 2007, **20**, 1903; (c) T. Netscher,Vitam. Horm., 2007, **76**, 155; (d) T. Netscher, F. Mazzini and R. Jestin, *Eur. J. Org. Chem.*, 2007, 1176.

2 (a) H. Dau and I. Zaharieva, *Acc. Chem. Res.* 2009, **42**, 1861; (b) C. Rein, P. Demel, R. A. Outten, T. Netscher and B. Breit, *Angew. Chem.*, Int. Ed., 2007, **46**, 8670; (c) A. Wildermann, Y. Foricher, T. Netscher and W. Bonrath, *Pure Appl. Chem.*, 2007, **79**, 1839; (d) W. Bonrath, M. Eggersdorfer and T. Netscher, *Catal. Today*, 2007, **121**, 45.

3 (a) P. Schudel, H. Mayer and O. Isler, in *The Vitamins*, ed. W. H. Sebrell and R. S. Harris, Academic, New York, 1972, vol. **5**, pp. 168–317; (b) W. Bonrath and T. Netscher, *Appl. Catal. A*, 2005, **280**, 55; (c) O. A. Kholdeeva, O. V. Zalomaeva, A. B. Sorokin, I. D. Ivanchikova, C. Della Pina and M. Rossi, *Catal. Today*, 2007, **121**, 58; (d) M. Eggersdorfer, D. Laudert, U. Letinois, T. McClymont, J. Medlock, T. Netscher and W. Bonrath, *Angew. Chem., Int. Ed.*, 2012, **51**, 12960.

4 (a) H. Sun, K. Harms and J. Sundermeyer, *J. Am. Chem. Soc*., 2004, **126**, 9550; (b) H. Sun, X. Li and J. Sundermeyer, *J. Mol. Catal. A*, 2005, **240**, 119; (c) K. Moller, G. Wienhofer, F. Westerhaus, K. Junge and M. Beller, *Catal. Today*, 2011, **173**, 68.

5 (a) L. F. Tietze, K. M. Sommer, J. Zinngrebe and F. Stecker, *Angew. Chem.* Int. Ed., 2005, **44**, 257; (b) G. Malaise, W. Bonrath, M. Breuninger and T. Netscher, *Helv. Chim. Acta*, 2006, 89, 797 – 812; (c) S. Bell, B. Wustenberg, S. Kaiser, F. Menges, T. Netscher and A. Pfaltz, *Science*, 2006, **311**, 642.

6 H. Verhagen , B. Buijsse, E. Jansen and B. Bueno-de-Mesquita, *Nutr. Today*, 2006, **41,** 244.

7 V. A. Bushmilyev, T. A. Kondratyeva, M. A. Lipkin, and A. V. Kondratyev, *Khim-Farm Zh.*,1991, **5**, 65. (In Russian)

8 (a) R. A. Sheldon and J. K. Kochi, 'Metal Catalyzed Oxidations of organic Compounds,' Academic Press, New York, 1981, p. 369. (b) T. Isshiki, T. Yui, H. Uno and M. Abe, Eur. Patent, 0127888, 1984; (c) R. Maasen, S. Krill and K. Huthmacher, Eur. Patent, 1132367, 2001; (d) K. Takehira, M. Shimizu, Y. Watanabe, H. Orita and T Hayakawa, *J. Chem. Soc. Chem. Comm*., 1989, 1705.

9 L. Schuster and H. Pommer, DE, 1793183, 1968.

10 (a) S. Ito, K. Aihara and M. Matsumoto, *Tetrahedron Lett.*, 1983, **24** 5249; (b) F. Shi, M. K. Tse and M. Beller, *Adv. Synth. Catal.*, 2007, **349**, 303; (c) G. Wienhofer, K. Schroder, K. Moller, K. Junge and M. Beller, *Adv. Synth Catal.*, 2010, **352**, 1615.

11 (a) M. Shimizu, K. Takehira, T. Hayakawa and H. Orita, *US. Pat.*, 1993, 5245059; (b) M. Vandewalle, WO. Patent, 1998, 18746.

12 (a) P. T. Anastas and J. C. Warner, Green Chemistry, Theory and Practice, Oxford University Press, Oxford, 1998; (b) Green Chemistry, Frontiers in Benign Chemical Syntheses and Processes, ed. P. T. Anastas and T. C. Williamson, Oxford University Press, Oxford, 1998; (c) J. Clark and D. Macquarrie, Blackwell, Handbook of Green Chemistry & Technology, ed. MA, 2002.

13 (a) C. W. Jones, Applications of Hydrogen Peroxide and Derivatives, Royal Society of Chemistry, Cambridge, 1999; (b) G. Strukul, Catalytic Oxidations with Hydrogen Peroxide as Oxidant ed., *Kluwer Academic*, Dordrecht, The Netherlands, 1992.

14 (a) P. T. Tanev, M. Chibwe and T. J. Pinnavaia, *Nature*, 1994, **368**, 321; (b) M. Taramasso, G. Perego and B. Notari, U.S. Patent 4 410 501, 1983; (c) B. Notari, *Adv. Catal.*, 1996, **41**, 253; (d) S. Gontier and A. Tuel, *Appl. Catal., A*, 1994, **118**, 173.

15 T. Hirao, *Chem. Rev.*,1997, **97**, 2707.

16 P. R. Makgwane and S. S. Ray, *Appl. Catal. A: Gen.*, 2015, **492**, 10.

17 P. S. Sonawane, S. S. Haram, P. R. Lawate, L. P. Kale, A. A Patil and P. S. Lokhande, *Int. J. Nano. Chem.*, 2015, **1**, 1.

18 R. Abazari, S. Sanati and L. A. Saghatforoush, *Chem. Engineering Journal*, 2014, **236**, 82.

19 A. L. Ahmad, B. Koohestani, S. Bhatia and S. B. Ooi, *Int. J. Appl. Ceram. Technol.*, 2012, **9**, 588.

20 E. T. Drew, Y. Yang, J. A. Russo, M. L. Campbell, S. A. Rackley, J. Hudson, P. Schmuki and D. C. Whitehead, *Catal. Sci. Technol.*, 2013, **3**, 2610.

21 D. P. Nair, T. Sakthivel, R. Nivea, J. S. Eshow and V. Gunasekaran, *J. Nanosci. Nanotechnol.*, 2015, **15**, 4392.

22 (a) Y. Segura, P. Cool, P. Van Der Voort, F. Mees, V. Meynen and E. F. Vansant, *J. Phys. Chem. B*, 2004, **108**, 3794; (b) S. Van Doorslaer, Y. Segura and P. Cool, *J. Phys. Chem. B*, 2004, **108**, 19404.

23 D. Zhao, J. Feng, Q. Huo, N. Melosh, G. H. Fredrickson, B.F. Chmelka and G.D. Stucky, *Science*, 1998, **279**, 548.

24 (a) C. K. P. Neeli, S. Ganji, V. S. P. Ganjala, R. R. S. Kamaraju and D. R. Burri, *RSC Adv.*, 2014, **4**, 14128; (b) C. K. P. Neeli, A. Narani, R. K. Marella, K. S. Rama Rao and D. R. Burri *Catal. Commun.*, 2013, **39**, 5; (c) A. Narani, K. H. P. Reddy, S. Vinukonda, K. S. Rama Rao and D. R. Burri, *Microporous Mesoporous Mater.*, 2011, **143**,132; (d) S. Ganji, S. Mutyala, C. K. P. Neeli, K. S. Rama Rao and D. R. Burri, *RSC Adv.*, 2013, **3**,11533.

25 J. E. Herrera, J. H. Kwak, J. Z. Hu, Y. Wang and C. H. F. Peden, *Top. Catal.*, 2006, **39**, 245.

26 (a) X. Gao, S. R. Bare, B. Meckhuysen and I. E. Wachs, *J. Phys. Chem. B*, 1998, **102,** 10842; (b) G. T. Went, S. T. Oyama and A. T. Bell, *J. Phys. Chem.*, 1990, **94**, 4240; (c) S. T. Oyama, G. T. Went, K. B. Lewis and A. T. Bell and G. A. Somorijai, *J. Phys. Chem.*, 1989, **93**, 6786. (d) Y. Segura, P. Cool, P. Kustrowski, L. Chmielarz, R. Dziembaj and E. F. Vansant, *J. Phys. Chem. B*, 2005, **109**, 12071.

27 (a) C. Hess, J. D. Hoefelmeyer and T. Don Tilley, *J. Phys. Chem.*, 2004, **108**, 9703; (b) C. Hess, M. H. Looi, S. B. A. Hamid and R. Schlogl, *Chem. Commun.*, 2006, 451; (c) C. J. Brinker, R. Kirkpatrick, D. R. Tallant, B. C. Bunker and B. J. Montez, *Non-Cryst. Solids*, 1988, **99**, 418.

28 N. N. Trukhan, V. N. Romannikov, E. A. Paukshtis, A. N. Shmakov and O. A. Kholdeeva, *J. Catal.*, 2001, **202**, 110.

29 O. A. Kholdeeva, I. D. Ivanchikova, M. Guidotti, N. Ravasio, M. Sgobba and M. V. Barmatova *Catal. Today*, 2009, **141**, 330.

30 O. A. Kholdeeva, M. S. Melgunov, A. N. Shmakov, N. N. Trukhan, V. V. Kriventsov, V. I. Zaikovskii, M. E. Malyshev and V. N. Romannikov, *Catal. Today*, 2004, **91-92**, 205.

31 O. A. Kholdeeva, I. D. Ivanchikova, M. Guidotti and N. Ravasio, *Green Chem.*, 2007, **9**, 731.

32 O. A. Kholdeeva, I. D. Ivanchikova, M. Guidotti, C. Pirovano, N. Ravasio, M. V. Barmatova, and Y. A. Chesalov, *Adv. Synth. Catal.*, 2009, **351**, 1877.

33 I. D. Ivanchikova, M. K. Kovalev, M. S. Melgunov, A. N. Shmakov and O. A. Kholdeeva, *Catal. Sci. Technol.*, 2014, **4**, 200.

34 I. D. Ivanchikova, N. V. Maksimchuk, R. I. Maksimovskaya, G. M. Maksimov and O. A. Kholdeeva, *ACS Catal.*, 2014, **4**, 2706.

V_2O_5/SBA-15 nanocatalysts for the selective synthesis of 2,3,5-trimethyl-1,4-benzoquinone at room temperature

Chinna Krishna Prasad Neeli, Venkata Siva Prasad Ganjala, Venkateswarlu Vakati, Kamaraju Seetha Rama Rao and David Raju Burri*

Graphical Abstract

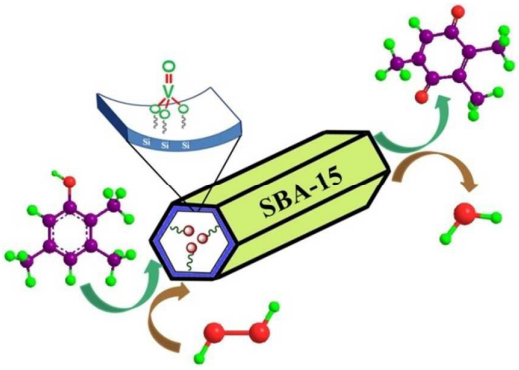

Molecular designed dispersion method yielded monodispersed nanoscale (4-7.5 nm sized) V_2O_5 dimeric species on SBA-15, which oxidized TMP into TMBQ with H_2O_2 under green conditions.